Charge order and antiferromagnetism in epitaxial ultrathin films of $EuNiO_3$

D. Meyers,[1,*] S. Middey,[1] M. Kareev,[1] Jian Liu,[2,†] J. W. Kim,[3] P. Shafer,[4] P. J. Ryan,[3] and J. Chakhalian[1]

[1]*Department of Physics, University of Arkansas, Fayetteville, Arkansas 72701, USA*

[2]*Materials Science Division, Lawrence Berkeley National Laboratory, Berkeley, California 94720, USA*

[3]*Advanced Photon Source, Argonne National Laboratory, Argonne, Illinois 60439, USA*

[4]*Advanced Light Source, Lawrence Berkeley National Laboratory, Berkeley, California 94720, USA*

(Received 15 August 2015; published 15 December 2015)

On a road towards applications and devices based on functional oxides with correlated electrons, the crucial element is uncovering the effects of the reduced dimensionality on the electronic phase transition into a multiordered ground state. Towards this goal, we present a study of reduced dimensionality on charge and antiferromagnetic orderings in ultrathin $EuNiO_3$ films on $NdGaO_3$ substrates using hard and soft resonant x-ray scattering to investigate the presence of electronic and magnetic orderings. Despite the ultrathin nature of the films, they exhibit the bulklike order parameters up to room temperature, suggesting that the spontaneously coherent Mott ground state in the highly distorted rare-earth nickelates can be successfully sustained even when constrained towards two-dimensionality. The presence of charge ordering at room temperature and below opens prospects for their use in novel electric-field-controlled devices.

DOI: 10.1103/PhysRevB.92.235126 PACS number(s): 68.35.Rh, 71.45.Lr, 75.50.Ee

I. INTRODUCTION

Transition-metal oxides (TMO) are host to a vast array of collective phenomena with enormous potential for use in next-generation electronic devices, including high-temperature superconductivity, colossal magnetoresistance, metal-insulator transition (MIT), orbital and charge ordering (CO) [1–5]. In particular, electric-field-induced changes in the CO state, where the modulated charge density acquires a periodic pattern typically leading to insulating behavior, have received wide attention lately and have been implemented in several devices [5–11]. In the ferrites, for instance, the application of an external electric field was found to induce a phase transition to a metallic state with a resistance change of several orders of magnitude, allowing their incorporation into devices [9–11]. These devices typically require ultrathin films or nanoparticles of materials, making the study of size effects of paramount importance to future functionality. For instance, it was found that the bulk CO transition is rapidly suppressed in the nanolimit or under high pressure for colossal magneto-resistance (CMR) manganite systems [12,13], while in thin films the CO transition temperature can be suppressed entirely or even increased from the bulk value [14–16]. Further, to be technologically viable a device typically needs to operate at room temperature and above, while in complex oxides CO is typically a low-temperature phenomenon. This has stimulated our search for materials that fulfill all of the criteria, i.e., display charge ordering, maintain this transition in nanometer-size applications, and operate at room temperature.

As a prototypical TMO perovskite system, the rare-earth nickelates with chemical formula $RNiO_3$ (R = Pr, Nd, Eu, Y, ...) incorporate Ni ions in a low spin $s = 1/2$ state and ionic $3d^7(t_{2g}^6 e_g)$ configuration, strongly covalent with oxygen, placing these systems firmly in the charge-transfer regime with a significant $3d^8\underline{L}$ component in the ground state [17,18]. This class of materials has received significant attention recently due to the MIT [17], E'-type antiferromagnetic transition (AFM) [19], structural transition [17], predicted high-T_c superconductivity [20], the potential for device applications [6,7,21], and the charge-ordering transition [22–26]. The charge-ordering transition, in particular, has been a source of controversy and still requires further insight [27–30]. Indeed, devices utilizing less distorted $NdNiO_3$ (NNO) have already been realized, including electric field control; however, the low transition temperature (~150 K) limits the practicality of such systems [7,18,21]. The rock-salt CO structure and the E'-type antiferromagnetic structure are shown in Fig. 1(a). In the rare-earth nickelates, the CO transition is invariably present in the bulk but, as in the manganites, has been shown to be suppressed in heteroepitaxial ultrathin films of RNO [24,27,29–31]. Specifically for NNO, it was found that the interface is able to "pin" the symmetry in the non-CO *Pbnm* state, analogous to the effect of surface strain in $La_{0.5}Ca_{0.5}MnO_3$ and Sr_2RuO_4 [12,29,30,32]. As changes in the ground state may render materials useless for applicability, it is important to find ways to mitigate the dimensionality effects. Within the nickelates, one possible route is the use of an R ion of smaller radius, which increases the distortion of the lattice and electron-phonon coupling and, correspondingly, the T_{MIT} at which CO arises in the bulk [17]. Determining whether this scheme can recover the typical bulk ground state or whether the two-dimensional geometry forbids its occurrence is crucial toward understanding the potential for this material to be used in future device applications.

In this paper, high-quality ultrathin films [14 unit cells (u.c.) ~5.3 nm] of $EuNiO_3$ (ENO) on $NdGaO_3$ (NGO) $(001)_{pc}$ substrates that feature moderate strain (~1.5%) and symmetry matching (*Pbnm*) were probed by resonant x-ray scattering (RXS) in the hard and soft x-ray regimes to determine the changes to the ground state due to the highly two-dimensional topology [33,34]. Structural diffraction confirmed that the film

*Present address: Department of Condensed Matter Physics and Materials Science, Brookhaven National Laboratory, Upton, New York 11973, USA; dmeyers@email.uark.edu

†Department of Physics and Astronomy, University of Tennessee, Knoxville, Tennessee 37996, USA.

was of high quality and consisted of a *single domain* in perfect registry with the substrate. Measurements of the $(011)_{or}$ [here *or* refers to orthorhombic structure; *pc* indicates pseudocubic] and $(\frac{1}{2}0\frac{1}{2})_{or}$ peaks at resonant edges were utilized to establish the presence of the bulklike CO and E'-type AFM orderings, respectively. Our results demonstrate that ENO films display bulklike multiordered ground states in sharp contrast to NNO, likely due to the larger distortion of the lattice and strong electron-phonon coupling destabilizing the substrate-induced symmetry pinning [35]. These findings increase the likelihood of fabricating multifunctional oxide-based devices employing room-temperature charge ordering.

II. EXPERIMENTAL METHODS

Ultrathin ENO samples were grown on NGO $(110)_{or}$ by pulsed laser deposition as described previously [36,37]. RXS measurements were performed at both the 4.0.2 beam line of the Advanced Light Source, Lawrence-Berkeley National Laboratory (soft RXS), and the 6-ID-B beam line of the Advanced Photon Source, Argonne National Laboratory. For the Ni L-edge, fluorescence and resonant diffraction data were measured simultaneously with separate regions of interest within a 2D detector.

III. RESULTS AND DISCUSSION

Figure 1(b) displays scans along the $(LL0)_{or}$ $[(00L)_{pc}]$ truncation rods with synchrotron-based diffraction. The structural quality is clearly evident from the appearance of Kiessig fringes spanning the $(110)_{or}$ truncation rod and film [37]. The spacing of the Kiessig fringes gives a film thickness of ~5.3 nm, corresponding to 14 u.c. of ENO, consistent with reflection high-energy electron diffraction (RHEED) oscillations during growth. The high photon flux of the synchrotron source is of particular importance due to the

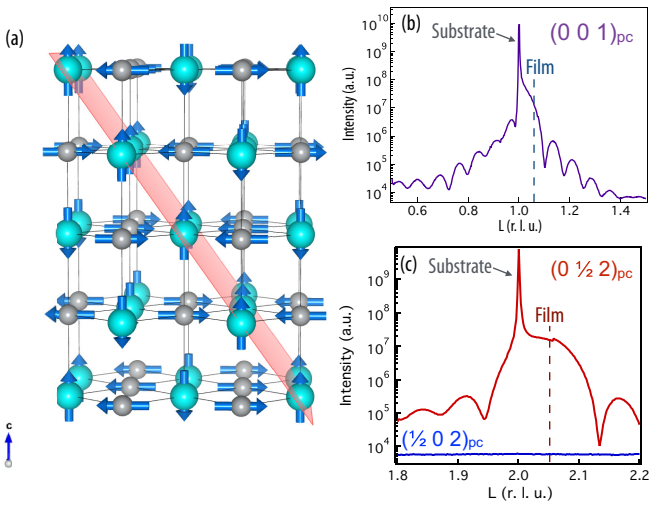

FIG. 1. (Color online) (a) Charge-ordered rock-salt crystal structure with exaggerated $Ni^{3\pm\delta}$ radius variations (Eu and O atoms omitted for clarity). A $(\frac{1}{2}0\frac{1}{2})_{or}$ E'-type antiferromagnetic plane is shown in red, with individual magnetic moment vectors for each Ni site. The *c* direction shown is the psuedocubic growth direction of the film. (b) *L* scan through the $(001)_{pc}$ truncation rods showing the high quality of the ultrathin films. (c) *L* scan around the $(0\frac{1}{2}2)_{pc}$ truncation rod.

relatively weak reflections used to probe CO. Beyond this, another basic indication of quality is the orientation of the orthorhombic *c* direction of the film relative to the substrate, which corresponds to a doubling of the pseudocubic unit cell. The NGO substrates used are cut to have the $(110)_{or}$ direction out of plane, giving primary in-plane directions of $(1\text{-}10)_{or}$ and $(001)_{or}$. We have defined the $(0K0)_{pc}$ direction to be parallel to the doubled orthorhombic *c* axis for both the substrate and film. Thus, there exists a half-order peak along the $(0K0)_{pc}$ direction but not along the $(H00)_{pc}$ direction corresponding to the orthorhombic *c* direction for both the substrate and film, indicating an untwinned film. Our scans across the $(0\frac{1}{2}2)_{pc}$ half-order peak show a clear substrate and film peak [Fig. 1(c)]. Subsequent attempts to locate the $(\frac{1}{2}02)_{pc}$ found no reflection. This indicates that there is no mixing of diffraction signatures from in-plane twinned orthorhombic domains. This point is crucial for investigating CO as domains with different *c* orientations will mix the reflected intensities from the $(H0L)_{or}$ and $(0KL)_{or}$ peaks [30], thus adding a large nonresonant scattering background which can obscure the resonant term.

Previous studies by several groups, including our recent work on NNO, have shown the E'-type AFM order in the nickelates is very robust and likely plays a significant role in the MIT transition in the less distorted nickelates [19,29,30,38]. In ENO, however, the separation of the MIT and the AFM transitions is nearly 300 K, allowing independent investigation of each. Note that the E'-type AFM ordering period contains four consecutive Ni moments along the $[111]_{pc}$ direction; thus this ordering can then be probed via the $(\frac{1}{2}0\frac{1}{2})_{or}$ peak $[(\frac{1}{4}\,\frac{1}{4}\,\frac{1}{4})_{pc}]$.

In Fig. 2(a) (inset), scans across the $(\frac{1}{4}\,\frac{1}{4}\,\frac{1}{4})_{pc}$ reflection revealed a strong peak at low temperature. The temperature dependence of the integrated intensity is shown in Fig. 2(a). As seen, a clear transition to the magnetically ordered state is found around 150 K. This is 55 K below the value reported in bulk, which is consistent with previously reported measurements on thin-film nickelates [17,39]. Here we stress that the magnetic Bragg peak corresponding to the bulklike E'-type AFM order was observed despite the ultrathin nature of the films, thereby displaying the robustness of this transition down to a thickness less than four full magnetic unit cells.

Having established the high-structural quality, single-domain phase, and the presence of the AFM transition, the temperature dependence of the $(0KL)_{or}$ peaks $[(-\frac{K}{2}\,\frac{L}{2}\,\frac{K}{2})_{pc}]$, associated directly with charge order, can be investigated [22–25]. Figure 3 shows the results of resonant energy scans around the $(011)_{or}$ peak. A clear energy dependence is observed at the Ni *K* edge with no apparent temperature dependence. The line shape has strong similarities with what was observed for thick and bulk NNO samples, with a small peak at higher energy (~8.36 keV) likely due to multiple scattering [22,23]. While the scattering around the Ni *K* edge is due to the resonant term of the total scattering factor, the off-resonance scattering indicates an additional contribution from the Thompson scattering off the Ni sites, whereas the Eu and O sites do not contribute by symmetry [22,23]. As with the resonant peak, no temperature dependence was observed for this contribution. Further analysis, taking the ratio of the peak at 8.348 keV to the background Thompson scattering (inset of Fig. 3), verifies the lack of any significant temperature

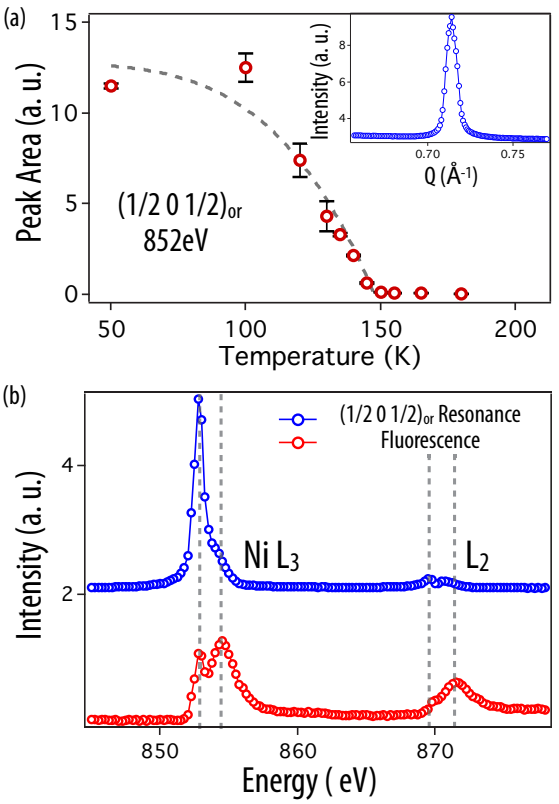

FIG. 2. (Color online) (a) Temperature dependence of the magnetic Bragg peak intensity corresponding to the magnetic order parameter. The inset shows the measured scattering at 50 K. (b) The 50 K resonant and fluorescence measurements of the Ni L_3 and L_2 edges. The fluorescence signal is enhanced 20 times, and the resonance data are vertically offset for clarity. Dashed lines are guides to the eye.

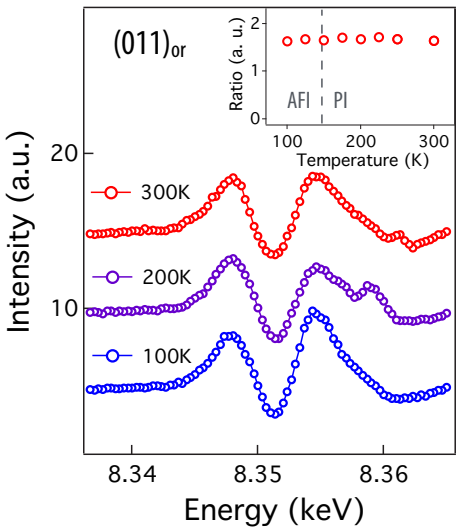

FIG. 3. (Color online) Resonant scattering at the $(011)_{or}$ peak at various temperatures. Data are offset for clarity. The inset shows the ratio of the peak around 8.348 keV to the background at 8.34 keV across the AFM transition up to room temperature (paramagnetic state inferred from bulk).

dependence for this peak. Upon cooling bulk ENO, the CO and MIT transitions initiate at ∼470 K [17,18]. In many films CO continues to develop with cooling, stabilizing at ∼100 K below the MIT [22]. Thus the absence of any temperature dependence here, ∼170 K below the bulk transition, is expected.

Having established that the temperature dependence of the $(011)_{or}$ peak indicates a bulklike CO transition, we next compare the charge disproportionation δ ($Ni^{3\pm\delta}$) of the film to the bulk. Low-temperature resonance scans at the $(\frac{1}{2}0\frac{1}{2})_{or}$ magnetic Bragg peak and the accompanying fluorescence background are shown in Fig. 2(b). The typical Ni L_3 and L_2 features are seen for the fluorescence data, with the higher-energy L_3 peak corresponding to the Ni^{3+} state around 855 eV and the lower-energy multiplet split peak, characteristic of the insulating state, around 853 eV, as also previously reported [37].

The resonance of the L_3 edge, besides indicating a strong Ni contribution to the observed magnetic Bragg peak, can reveal the degree of charge disproportionation $Ni^{3\pm\delta}$ in the sample [19,38,40]. Specifically, Scagnoli *et al.* used a configuration interaction model to demonstrate that the value of δ strongly influences the line shape of the resonant peak [38,41]. Surveying the available compounds, Bodenthin *et al.* found, for $RNiO_3$ *powder* samples spanning several rare-earth ions, no deviation in the magnitude of δ [19]. This result is quite surprising as the degree of the monoclinic distortion increases with decreasing rare-earth radius, and this was expected to increase the value of δ. For our ENO ultrathin films, the line shape for the σ incident light is nearly identical to what was observed for the bulk samples and, based upon the similarity with the calculated spectra of $\delta = 0.32e$ from Ref. [19], is within the $0.05e$ range found for all the $RNiO_3$ bulk powder compounds. Combining the results of the $(011)_{or}$ CO peak and the $(\frac{1}{2}0\frac{1}{2})_{or}$ magnetic peak, it is therefore clear that the CO in the ENO film maintains a bulklike value despite the highly constraining two-dimensional geometry in sharp contrast to the lattice pinning found for NNO thin films [29,30].

Thus we find the higher distortion in this nickelate incorporating a smaller rare-earth ion, Eu, is able to recover the bulklike phase transitions that were suppressed for NNO in the same two-dimensional geometry [39,42]. Previous work on rare-earth nickelate thin films showed that a heterointerface with the substrate can readily suppress the monoclinic symmetry, bulklike CO, and the MIT transitions under compressive strain [7,27,43–46]. Further, some films have been found to maintain a MIT and yet show no symmetry breaking on crossing the MIT [27,29,30]. We conclude that the higher distortion and stronger electron-phonon coupling in ENO allows CO to persist in the insulating, tensile-strained sample despite the ultra thin motif. Moreover, it is quite remarkable that, based upon the line shape of the Ni L_3-edge resonant scattering, the degree of charge disproportionation appears unchanged from the bulk value based upon the resonance at the $L_{3,2}$ edges [19]. We have therefore uncovered a mechanism to overcome the suppression of bulk functional properties that has been observed previously in other nickelate films.

In conclusion, we synthesized ultrathin films of ENO films on NGO substrates to investigate the stability of the AFM and CO orderings against the ultrathin geometry via hard and soft XRS. An AFM transition is found to occur near the expected

temperature with the Q value corresponding to the bulklike E'-type ordering. Interestingly, the magnitude of the CO δ parameter, derived from magnetic scattering, was found to be approximately the same as that reported for both bulk and thick films of various $R\mathrm{NiO}_3$. Thus in ENO, despite the ultrathin geometry and altered electronic bandwidth, our findings revealed that the CO and AFM transitions remain bulklike. Moreover, CO is observed at room temperature, rendering ultrathin ENO films and heterojunctions potentially useful for novel electric-field-controlled devices along with CMR manganites and ferrites [5–11].

ACKNOWLEDGMENTS

The authors deeply acknowledges numerous fruitful theory related discussions with Andrew Millis, Priya Mahadevan, Daniel Khomskii, and D. D. Sarma. J.C. was supported by the Department of Energy Grant No. DE-SC0012375 for synchrotron work. M.K. And D.M. were supported by Gordon and Betty Moore Foundation EPiQS Initiative through Grant No. GBMF4534 for synthesis effort. J.L. and S.M. were supported by the DOD-ARO under Grant No. 0402-17291. J.L. is sponsored by the Science Alliance Joint Directed Research and Development Program at the University of Tennessee. The Advanced Light Source is supported by the Director, Office of Science, Office of Basic Energy Sciences, of the U.S. Department of Energy under Contract No. DE-AC02-05CH11231. This research used resources of the Advanced Photon Source, a U.S. Department of Energy (DOE) Office of Science User Facility operated for the DOE Office of Science by Argonne National Laboratory under Contract No. DE-AC02-06CH11357.

[1] J. Chakhalian, J. W. Freeland, H.-U. Habermeier, G. Cristiani, G. Khaliullin, M. van Veenendaal, and B. Keimer, Science **318**, 1114 (2007).
[2] J. Chakhalian, J. W. Freeland, G. Sprajer, J. Strempfer, G. Khaliullin, J. C. Cezar, T. Charlton, R. Dalgliesh, C. Bernhard, G. Cristiani, H.-U. Habermeier, and B. Keimer, Nat. Phys. **2**, 244 (2006).
[3] J. Chakhalian, A. J. Millis, and J. Rondinelli, Nat. Mater. **11**, 92 (2012).
[4] M. Imada, A. Fujimori, and Y. Tokura, Rev. Mod. Phys. **70**, 1039 (1998).
[5] A.-M. Haghiri-Gosnet and J.-P. Renard, J. Phys. D **36**, R127 (2003).
[6] C. H. Ahn, J.-M. Triscone, and J. Mannhart, Nature (London) **424**, 1015 (2003).
[7] R. Scherwitzl, P. Zubko, I. Gutierrez Lezama, S. Ono, A. F. Morpurgo, G. Catalan, and J.-M. Triscone, Adv. Mater. **22**, 5517 (2010).
[8] S. Zhou, Y. Guo, J. Zhao, L. He, C. Wang, and L. Shi, J. Phys. Chem. C **115**, 8989 (2011).
[9] K. Fujiwara, T. Hori, and H. Tanaka, J. Phys. D **46**, 155108 (2013).
[10] S. Lee, A. Fursina, J. T. Mayo, C. T. Yavuz, V. L. Colvin, R. G. Sumesh Sofin, I. V. Shvets, and D. Natelson, Nat. Mater. **7**, 130 (2008).
[11] Han-Chun Wu, O. N. Mryasov, M. Abid, K. Radican, and I. V. Shvets, Sci. Rep. **3**, 1830 (2013).
[12] T. Sarkar, B. Ghosh, A. K. Raychaudhuri, and T. Chatterji, Phys. Rev. B **77**, 235112 (2008).
[13] D. P. Kozlenko, Z. Jirak, and B. N. Savenko, J. Phys. Condens. Matter **16**, 5883 (2004).
[14] C. K. Xie, J. I. Budnick, W. A. Hines, B. O. Wells, F. He, and A. R. Moodenbaugh, Phys. Rev. B **77**, 201403(R) (2008).
[15] A. Maniwaa, K. Okanoa, I. Ohkuboa, H. Kumigashiraa, M. Oshimaa, M. Lippmaab, M. Kawasakic, and H. Koinumad, J. Magn. Magn. Mater. **310**, 2237 (2007).
[16] Z. Q. Yang, Y. Q. Zhang, J. Aarts, M.-Y. Wu, and H. W. Zandbergen, Appl. Phys. Lett. **88**, 072507 (2006).
[17] M. Luisa Medarde, J. Phys. Condens. Matter **9**, 1679 (1997).
[18] G. Catalan, Phase Transitions **81**, 729 (2008).
[19] Y. Bodenthin, U. Staub, C. Piamonteze, M. García-Fernández, M. J. Martínez-Lope, and J. A. Alonso, J. Phys. Condens. Matter **23**, 036002 (2011).
[20] J. Chaloupka and G. Khaliullin, Phys. Rev. Lett. **100**, 016404 (2008).
[21] W. L. Lim, E. J. Moon, J. W. Freeland, D. J. Meyers, M. Kareev, J. Chakhalian, and S. Urazhdin, Appl. Phys. Lett. **101**, 143111 (2012).
[22] U. Staub, V. Scagnoli, A. M. Mulders, K. Katsumata, Z. Honda, H. Grimmer, M. Horisberger, and J. M. Tonnerre, Phys. Rev. B **71**, 214421 (2005).
[23] J. E. Lorenzo, J. L. Hodeau, L. Paolasini, S. Lefloch, J. A. Alonso, and G. Demazeau, Phys. Rev. B **71**, 045128 (2005).
[24] V. Scagnoli, U. Staub, M. Janousch, A. M. Mulders, M. Shi, G. I. Meijer, S. Rosenkranz, S. B. Wilkins, L. Paolasini, J. Karpinski, S. M. Kazakov, and S. W. Lovesey, Phys. Rev. B **72**, 155111 (2005).
[25] V. Scagnolia, U. Staub, M. Janousch, G. I. Meijer, L. Paolasinic, F. D'Acapito, J. G. Bednorz, and R. Allenspach, J. Magn. Magn. Mater. **272-276**, 420 (2004).
[26] S. Yamamoto and T. Fujiwara, J. Phys. Soc. Jpn. **71**, 1226 (2002).
[27] M. Hepting, M. Minola, A. Frano, G. Cristiani, G. Logvenov, E. Schierle, M. Wu, M. Bluschke, E. Weschke, H.-U. Habermeier, E. Benckiser, M. Le Tacon, and B. Keimer, Phys. Rev. Lett. **113**, 227206 (2014).
[28] M. Wu, E. Benckiser, P. Audehm, E. Goering, P. Wochner, G. Christiani, G. Logvenov, H.-U. Habermeier, and B. Keimer, Phys. Rev. B **91**, 195130 (2015).
[29] D. Meyers, J. Liu, J. W. Freeland, S. Middey, M. Kareev, J. Kwon, J. M. Zuo, Y.-D. Chuang, J.-W. Kim, P. J. Ryan, and J. Chakhalian, arXiv:1505.07451.
[30] M. H. Upton, Y. Choi, H. Park, J. Liu, D. Meyers, J. Chakhalian, S. Middey, J.-W. Kim, and P. J. Ryan, Phys. Rev. Lett. **115**, 036401 (2015).
[31] R. Lengsdorf, A. Barla, J. A. Alonso, M. J. Martinez-Lope, H. Micklitz, and M. M. Abd-Elmeguid, J. Phys. Condens. Matter **16**, 3355 (2004).
[32] R. Matzdorf, Z. Fang Ismail, J. Zhang, T. Kimura, Y. Tokura, K. Terakura, and E. W. Plummer, Science **289**, 746 (2000).

[33] J. Fink, E. Schierle, E. Weschke, and J. Geck, Rep. Prog. Phys. **76**, 056502 (2013).
[34] J.-L. Hodeau, V. Favre-Nicolin, S. Bos, H. Renevier, E. Lorenzo, and J.-F. Berar, Chem. Rev. **101**, 1843 (2001).
[35] H. Y. Qi, M. K. Kinyanjui, J. Biskupek, D. Geiger, E. Benckiser, H.-U. Habermeier, B. Keimer, and U. Kaiser, J. Mater. Sci. **50**, 5300 (2015).
[36] D. Meyers, E. J. Moon, M. Kareev, I. C. Tung, B. A. Gray, J. Liu, M. J. Bedzyk, J. W. Freeland, and J. Chakhalian, J. Phys. D **46**, 385303 (2013).
[37] D. Meyers, S. Middey, M. Kareev, M. van Veenendaal, E. J. Moon, B. A. Gray, J. Liu, J. W. Freeland, and J. Chakhalian, Phys. Rev. B **88**, 075116 (2013).
[38] V. Scagnoli, U. Staub, A. M. Mulders, M. Janousch, G. I. Meijer, G. Hammerl, J. M. Tonnerre, and N. Stojic, Phys. Rev. B **73**, 100409(R) (2006).
[39] Jian Liu, M. Kargarian, M. Kareev, B. Gray, P. J. Ryan, A. Cruz, N. Tahir, Y.-D. Chuang, J. Guo, J. M. Rondinelli, J. W. Freeland, G. A. Fiete, and J. Chakhalian, Nat. Commun. **4**, 2714 (2013).
[40] V. Scagnoli, U. Staub, Y. Bodenthin, M. García-Fernández, A. M. Mulders, G. I. Meijer, and G. Hammerl, Phys. Rev. B **77**, 115138 (2008).
[41] F. de Groot, Coord. Chem. Rev. **249**, 31 (2005).
[42] J. Chakhalian, J. M. Rondinelli, J. Liu, B. A. Gray, M. Kareev, E. J. Moon, N. Prasai, J. L. Cohn, M. Varela, I. C. Tung, M. J. Bedzyk, S. G. Altendorf, F. Strigari, B. Dabrowski, L. H. Tjeng, P. J. Ryan, and J. W. Freeland, Phys. Rev. Lett. **107**, 116805 (2011).
[43] J. Son, P. Moetakef, J. M. LeBeau, D. Ouellette, L. Balents, S. J. Allen, and S. Stemmer, Appl. Phys. Lett. **96**, 062114 (2010).
[44] Y. Kumar, R. J. Choudhary, and R. Kumar, Appl. Phys. Lett. **101**, 132101 (2012).
[45] D. Kaur, J. Jesudasan, and P. Raychaudhuri, Solid State Commun. **136**, 369 (2005).
[46] A. S. Disa, D. P. Kumah, J. H. Ngai, E. D. Specht, D. A. Arena, F. J. Walker, and C. H. Ahn, APL Mater. **1**, 032110 (2013).